Journal of the Korean Society of Oceanography
Vol. 37, No. 1, pp. 1 — 9 March 2002

# Tidal variations in the cable voltage across the Korea Strait

SANG JIN LYU*, YOUNG-GYU KIM[1], KUH KIM*, JEFFREY W. BOOK[2] AND BYUNG HO CHOI[3]
*OCEAN Lab., School of Earth and Environmental Sciences, Seoul National University, Seoul 151-742, Korea
[1]Naval Systems R&D Center, Agency for Defense Development, Chinhae 645-600, Korea
[2]Naval Research Laboratory, Stennis Space Center, MS 39529, USA
[3]Department of Civil Engineering, Sung Kyun Kwan University, Suwon 440-746, Korea

Cable voltage was measured simultaneously at Hamada, Japan and Pusan, Korea, using an in-service telephone cable from March to December 1990. The spectral and harmonic analyses of these data sets show that tidal signals are dominant, and that tidal constituents $M_2$ and $O_1$, which are not affected by solar geomagnetic variations, have almost the same amplitude and are of opposite phase to each other. Comparing the voltage difference in 1990 with that measured using the now abandoned cable in 1998, there are dominant tidal signals at the same periods in both data sets. They have approximately the same amplitude and phase for $M_2$ and $O_1$. The relationship between the observed voltage and the volume transport through the Korea Strait can be considered robust and stable over time. The conversion factor from voltage to transport is estimated to be $11.9\times10^6$ $m^3s^{-1}volt^{-1}$ by comparing the amplitude of model-derived $M_2$ tidal transport with that of the voltage difference in 1998. This value changes to $8.6\times10^6$ $m^3s^{-1}volt^{-1}$ when taking into consideration the horizontal electric current effect. This effect depends on the downstream length scale of the flow. To obtain a more reliable and stable conversion factor from voltage to transport, the voltage should be compared with observed sub-tidal transports, which may have long downstream length scales.

**Key words:** the Korea Strait, cable voltage, tide, transport

## 1. INTRODUCTION

Electromotive force is induced according to Faraday's Law when seawater with electric conductivity flows under geomagnetic fields. These motion-induced electric potential differences have been used to estimate the volume transport through a strait. Longuet-Higgins (1949) introduced this method and Bowden (1956) applied it to the Dover Strait. Also, Larsen (1992) has successfully monitored the volume transport through the Florida Strait.

Such a method has been applied to the Korea Strait using the in-service submarine telephone cable between Pusan, Korea and Hamada, Japan (Fig. 1). The voltage was measured separately at each of the ground sites, Hamada and Pusan. Kawatate *et al.* (1991) examined the relationship between the voltage measured at Hamada from July 1987 to February 1988 and current data measured near Tsushima Island in 1987. They found that the energy in both data sets is concentrated in tidal frequencies and that there are high coherencies at those frequencies. They concluded that the observed voltage is related to the motion of seawater. Choi *et al.* (1992) used the voltage measured at Pusan from March 1990 to March 1991 and current data measured close to the midpoint of the cable and sea level data at Pusan. They showed that all data possess high spectral energies at low and tidal frequencies. By comparing the amplitude of the $M_2$ signal in the measured voltage with that of $M_2$ tidal transport from a tidal model, they obtained a voltage to transport conversion factor of $35.95\times10^6$ $m^3s^{-1}volt^{-1}$ (Table 1). Choi *et al.* (1997) also investigated the cable voltage measured at Pusan from March 1990 to September 1996. Spectral analyses showed that tidal components are dominant. For this period, the conversion factor was $30.90\times10^6$ $m^3s^{-1}volt^{-1}$ (Table 1). The previous studies in the Korea Strait used the voltage measured at a single site between the power-supply cable and the ground (Fig. 2a). These studies did not thoroughly analyze the voltage differences measured simultaneously at Pusan and Hamada.

*Corresponding author: sjlyu@ocean.snu.ac.kr

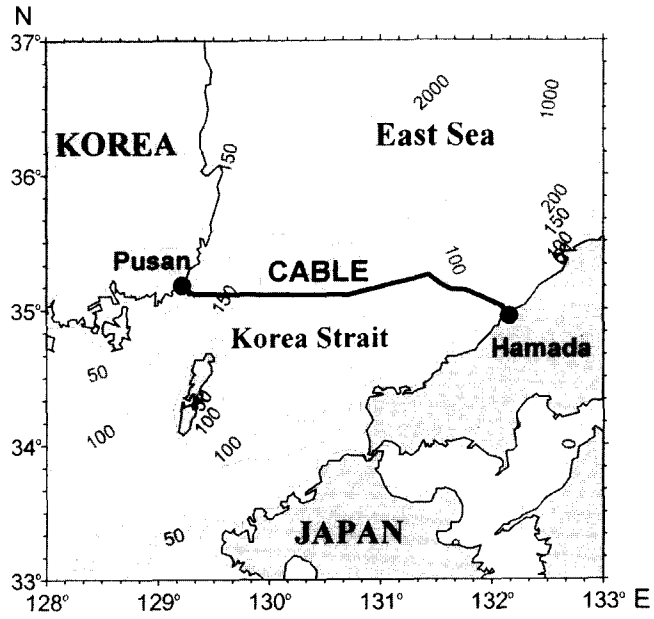


**Fig. 1.** Arrangement of the submarine cable between Pusan and Hamada and the bottom topography in meters.

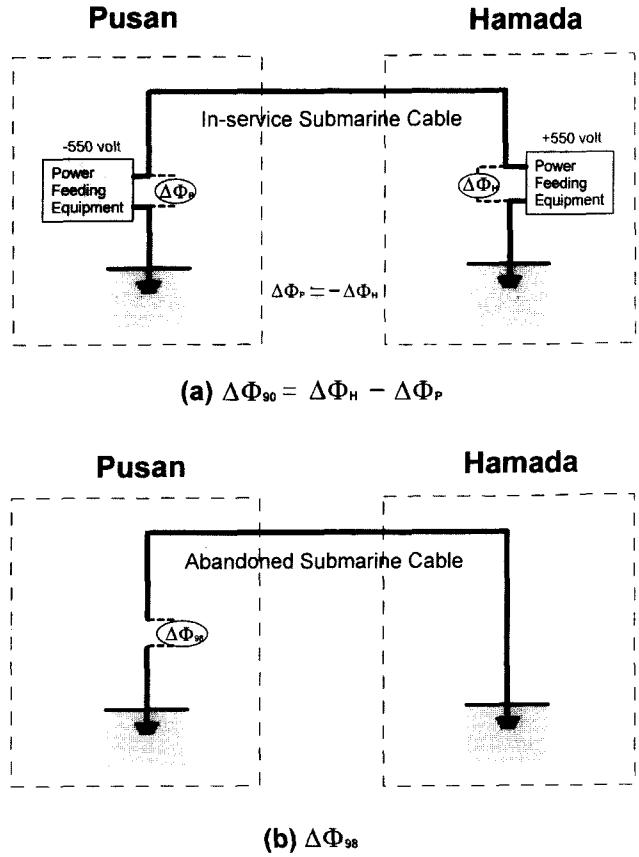


**Fig. 2.** Schematic diagrams of the cable voltage measurement at Pusan and Hamada for (a) the in-service cable and for (b) the abandoned cable.

As a new optical fiber cable was established for communication in July 1997, the abandoned telephone cable was transferred to RIO (Research Institute of Oceanography, Seoul National University) and ORI (Ocean Research Institute, University of Tokyo) from Korea Telecom and NTT of Japan, respectively, as part of a cooperative research program of NEAR-GOOS (NorthEast Asian Region Global Ocean Observing System). Thereafter, since March 1998, the motion-induced electric potential difference between Pusan and Hamada has been measured at the Pusan Submarine Relay Station using the abandoned cable (Fig. 2b).

The characteristics of the motion-induced voltage are considered theoretically in this paper. These theoretical characteristics are to be found in tidal variations of the voltages measured simultaneously at Pusan and Hamada using the in-service cable in 1990. The voltage difference between Pusan and Hamada measured in 1990 is compared with the voltage difference measured using the abandoned cable in 1998. The conversion factor from voltage to transport is then estimated from tidal signals.

## THEORY

As a simple case (Fig. 3a) we assume that there is no spatial variation of velocity in a strait. The conductivities ($\sigma_1$, $\sigma_2$) of water and upper crust, the geomagnetic field, the width of the strait and the depths

**Table 1.** Conversion factors from voltage to transport, which are estimated by comparing the amplitude of model-derived tidal transport with that of tidal variation in voltage. The values within parentheses denote voltages and conversion factors when taking into consideration the horizontal electric current effect.

| Study | Tidal constituent | Tidal transport ($10^6$ m$^3$s$^{-1}$) | Voltage (volt) | Conversion factor ($10^6$ m$^3$s$^{-1}$volt$^{-1}$) |
|---|---|---|---|---|
| Choi *et al.* (1992) | $M_2$ | 5.5 | 0.154 | 35.95 |
| Choi *et al.* (1997) | $M_2$ | 5.5 | 0.178 | 30.90 |
| This study | $M_2$ | 4.38 | 0.369 (0.51) | 11.9 (8.6) |
| | $O_1$ | 1.79 | 0.122 (0.17) | 14.7 (10.5) |

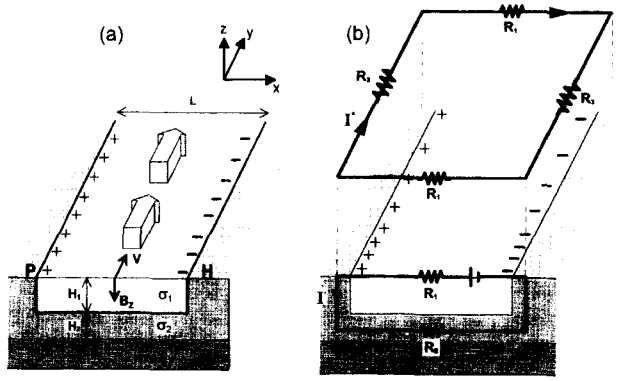


**Fig. 3.** (a) Schematic diagram of motion-induced voltage across a strait and (b) a circuit model across vertical and horizontal sections.

($H_1$, $H_2$) of water and upper crust are also assumed constant. When electric conductive seawater ($\sigma_1 = 4$ ~5 S m$^{-1}$ in general) moves through the geomagnetic field, an electromotive force ($\varepsilon$) is induced by Faraday's Law,

$$\varepsilon = \vec{B} \cdot \vec{L} \times \vec{V}, \tag{1}$$

where, $\vec{B}$ is the geomagnetic field, $\vec{L}$ is the distance vector, and $\vec{V}$ is the velocity of the water.

By this electromotive force positive charges are pushed to the left-hand side and negative ones to the right-hand side when the seawater moves in the positive $y$ direction (Fig. 3a). This causes an electric potential difference across the strait, $\Delta\phi$,

$$\Delta\phi = B_z L v, \tag{2}$$

where $B_z$ is the vertical geomagnetic field (<0), $L$ is the width of the strait, and v is the speed of the current in the y direction. When v is positive, a higher electric potential at $P$ is induced than at $H$ in Fig. 3a. Since the water depth $H_1$ is assumed constant, the induced potential difference is proportional to the volume transport through the strait. In such a simple case the separated charges are evenly distributed along the strait. The variations of the electric potential at any two points across the strait must have the same amplitude and opposite phase.

The upper crust has a small electric conductivity ($\sigma_2$), which allows the completion of a circuit in the vertical section (Fig. 3b). The electric potential gradient can be described as follows according to Sanford and Flick (1975).

$$\nabla\phi = \vec{v} \times \vec{B} - \vec{J}/\sigma_1 \tag{3}$$

and

$$\vec{J}/\sigma_1 = \nabla \times \int_z^{\zeta} B_z(\vec{v} - \overline{v^*})dz' + \frac{\overline{D}}{2\pi D} \nabla \times \hat{k} \int_{-\infty}^{\infty} \int_{-\infty}^{\infty} \nabla \cdot B_z \overline{v^*} \ln r dx' dy' \tag{4}$$

where $\vec{j}$ is electric current density. $D$ is defined as $D = H_1 + \frac{\sigma_2}{\sigma_1} H_2$ and $D$ is the regional average of $D$ over area of roughly $L^2$ size. $\overline{v^*}$ is the conductivity-weighted velocity defined as $\overline{v^*} = \frac{1}{D}\int_{-H_1}^{0} \vec{v} dz$. $\vec{k}$ is the unit vector in the $z$ direction and $r = ((x-x')^2+(y-y')^2)^{1/2}$.

The first and second terms in the right hand side of (4) indicate the electric current through the vertical section and through the horizontal section, respectively. In general, the former is much larger than the latter (Sanford and Flick, 1975). First considering the electric current through the vertical section, the potential gradient in the $x$ direction is

$$\frac{\partial \phi}{\partial x} = B_z \overline{v^*} \tag{5}$$

That is, the potential difference is dependent on the vertically averaged and conductivity-weighted velocity. Since the conductivities of the seawater and the upper crust have little variation, the local motion-induced potential difference across the strait can be simplified to

$$\Delta\phi_L = \frac{\sigma_1 H_1}{\sigma_1 H_1 + \sigma_2 H_2} B_z L v$$
$$= v_0 B_z L v \tag{6}$$

where $v_0 = \frac{\sigma_1 H_1}{\sigma_1 H_1 + \sigma_2 H_2}$.

Since we assume no spatial variations, the variations of the electric potential at any two points across the strait have the same amplitude and opposite phases.

The electric current through the horizontal section also affects the potential difference, when there are downstream changes in the conductivities ($\sigma_1$, $\sigma_2$) of water and upper crust, or the velocity ($v$), or the depths ($H_1$, $H_2$) of water and upper crust. These effects are related to the spatial distribution of $\nabla \cdot \overline{v^*}$ as shown in the second term in the right hand side of (4) and the relation is given by

$$\nabla \cdot \overline{v^*} = -\frac{1}{D}\frac{\partial \zeta}{\partial t} - \frac{\overline{v^*}}{D} \cdot \nabla D, \tag{7}$$

where $\zeta$ is sea surface elevation. The amount of the separated charges along the strait is determined by

the local time variation of the sea surface and the spatial distribution of velocity, conductivity, and depth. If the separated electric charges are unevenly distributed along the strait as in Fig. 3b, an electric current through the horizontal section is induced. Then the electric potential difference across the strait is reduced from the local potential difference ($\Delta\Phi_L$). The variations of the electric potential at any two given points across the strait may have different amplitudes from each other. Moreover, the cross-stream potential differences can be different even though the volume transports through each vertical section are the same.

A circuit model as shown in Fig. 3b is introduced to analyze the effect of the horizontal electric current. With the characteristic length scale of the stream in the $y$ direction $Y$, resistances can be estimated as follows (Larsen, 1992).

$$R_1 = 2L/(Y\sigma_1 H_1)$$

$$R_2 = 2L/(Y\sigma_2 H_2)$$

$$R_3 = \pi/2\tau^*, \quad (8)$$

where $R_1$, $R_2$ and $R_3$ are the resistances of ocean, upper crust, and land, respectively, and $\tau^*$ is the conductance of the land. The potential difference across the strait induced by the local volume transport ($\Delta\Phi_L$) is reduced by the effect of the horizontal electric current ($\Delta\Phi_I$),

$$\phi_V = \Delta\phi_L + \Delta\phi_I = (1-x)\Delta\phi, \quad (9)$$

where $x = v_0 R_1/R_3\ (1+v_0 R_1/R_3)^{-1}$. If $R_3$ is reduced to 0, $\kappa$ becomes close to 1; that is, the horizontal electric current ($I^*$) completely shorts out the cross-stream potential difference ($\Delta\Phi_V$). As $R_3$ increases, $\kappa$ nears 0 and the effect of $I^*$ become negligible. $\Delta\Phi_I$ also becomes small when $v_0$ is small; that is, the conductance of the upper crust is large or $Y$ is much larger than $L$.

Horizontal geomagnetic variations can also affect the cross-stream potential difference (Larsen *et al.*, 1996). However, these effects are dominant at short periods, especially in the bands of solar diurnal variations around frequencies such as 1, 2, 3, and 4 cpd (Larsen, 1992). The tidal constituents $K_1$ and $P_1$ in the diurnal band and $S_2$ and $K_2$ in the semidiurnal band lie within these bands. However, the constituents $O_1$ and $M_2$ lie well outside the solar geomagnetic bands (Mayer and Larsen, 1986). Since only the $M_2$ and $O_1$ tidal constituents are discussed in this study, the geomagnetic effects need not be considered.

The variations of the electric potential on each side of the strait are complicated by the temporal variation of the sea surface and the downstream change of velocity, conductivity, and water depth. The ground sites of the cable between Pusan and Hamada are not on opposite sides of the general flow in the Korea Strait and the bottom topography is not simple along the strait (Fig. 1). To investigate whether the observed voltage between Pusan and Hamada has the same characteristics as in a simple theoretical case and how much other factors besides volume transport affect the voltage, it is necessary to compare amplitudes and phases of voltages measured simultaneously at the two ground sites of the cable.

## DATA AND ANALYSIS

### *Voltages measured simultaneously at Pusan and Hamada in 1990*

Voltage was measured simultaneously at Pusan and Hamada from March to December 1990. Electric power was supplied to the cable in such a way that the electric potentials to the ground were near -550 and +550 volt at Pusan and Hamada, respectively. The exact potential difference values depend on the volume and character of the flow of seawater into the East Sea through the Korea Strait. However, it was reported by Bahk (1991) that the voltmeter installed at Pusan is affected by room temperature variation and that this effect is as large as ±2 volt. Unfortunately, it is impossible to correct the temperature dependency because temperature was not measured. Moreover, the supplied power itself had long-term variations as well as abrupt changes. These various effects prevent a meaningful long-term analysis of voltage data, and thus this study concentrates on tidal variations.

The voltage-sampling interval was 2.5 minutes at Hamada and 1 minute at Pusan. To remove short-term variations, measured voltages were low-pass filtered with a cut-off period of 1.143 hours and a half-power period of 2 hours. Fig. 4 shows the amplitude response function of this filter. Filtered data were subsampled every hour as shown in Fig. 5. There is an abrupt voltage change as large as 1 volt at Hamada (Fig. 5a) in July 1990 that may be related to the change of the supplied power. The voltage at Pusan (Fig. 5b) has a long-term variation as large

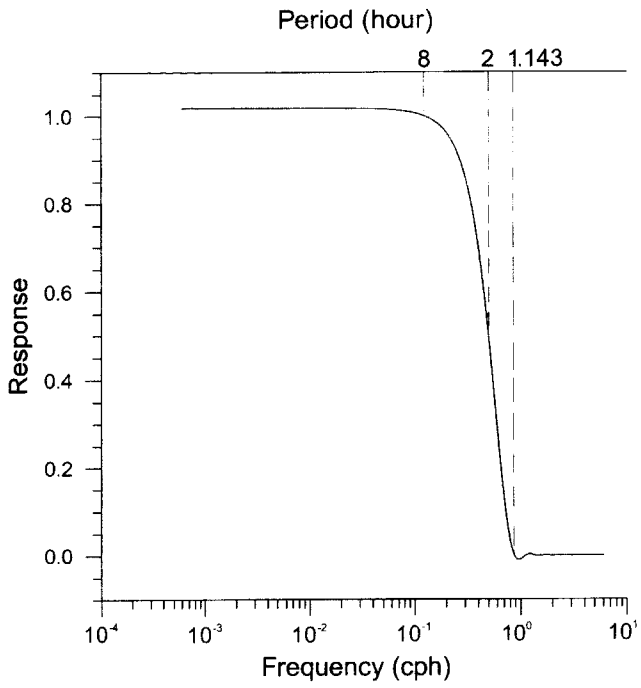


**Fig. 4.** Frequency response function of a low-pass filter with a half-power period of 2 hours and a cut-off period of 1.143 hours.

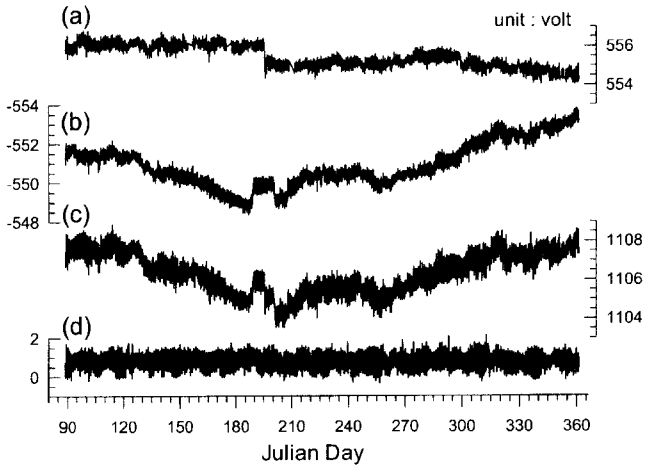


**Fig. 5.** Time series of voltages measured simultaneously at (a) Hamada and (b) Pusan by using the in-service submarine cable in 1990, and (c) the difference between them ($\Delta\Phi_{90}$). (d) is voltage difference ($\Delta\Phi_{98}$) measured at Pusan by using the abandoned cable in 1998.

as 5 volt that may be related to the long-term variation of the room temperature (Bahk, 1991). However, the short-term variations in both signals have about the same range of variation of up to 1 volt. A six-day segment of voltage time series is shown in Fig. 6. There are manifest semi-diurnal and diurnal variations as large as 0.5 volt at Hamada (Fig. 6a)

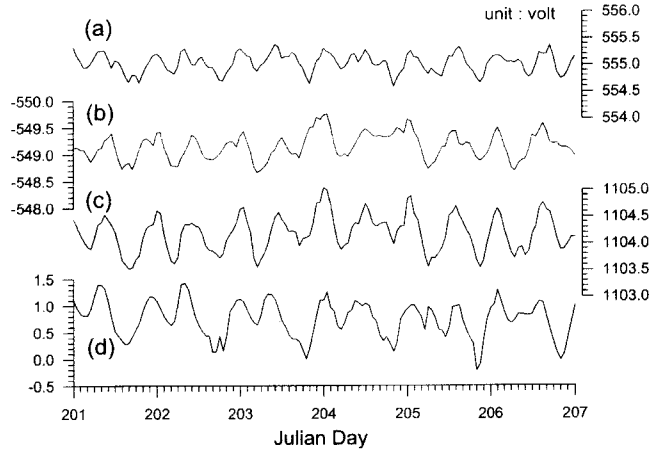


**Fig. 6.** As in Fig. 5 except for a six-day sample time series.

and Pusan (Fig. 6b), which explain most of the short-term variations in Fig. 5.

Power spectral analyses (Fig. 7) also indicate that both spectra have peaks at the same diurnal (A: 25 h 38.82 m, B: 23 h 46.91 m), semi-diurnal (C: 12 h 27.43 m), and 1/3-day (D: 8 h 1.47 m) periods. They have almost the same magnitudes at each peak. The variation with 1/3-day period may be related to solar geomagnetic variations (Larsen, 1992). The coherency and cross-phase spectra between the voltages measured simultaneously at Hamada and Pusan are shown in Fig. 8. Coherencies are higher than the 95% confidence level only at diurnal (A, B), semidiurnal (C), and 1/3-day (D) periods. The cross-phase spectra have values near 180° at those periods. These values are 182° at A, 175° at B, 182° at C, and 179° at D. It can be inferred from these coherency and cross-phase spectra that the voltages measured simultaneously at Hamada and Pusan have phase differences of about 180° at tidal periods, where most energy is concentrated.

To further establish that such a phase relation exists and to compare tidal amplitudes, harmonic analyses were performed. Considering data intermittence and the abrupt changes that occurred in July 1990, all the data are divided into seven 29-day long sets. The constituents used in these harmonic analyses are the 27 standard constituents that are generally used for 29-day long data. Among them, the constituents related to the solar diurnal variations such as $K_1$ and $S_2$ can be contaminated by horizontal geomagnetic variations as reported by Larsen (1992). The major constituents that are not related to the geomagnetic effects are $M_2$ and $O_1$ (Table 2, 3). The mean $M_2$

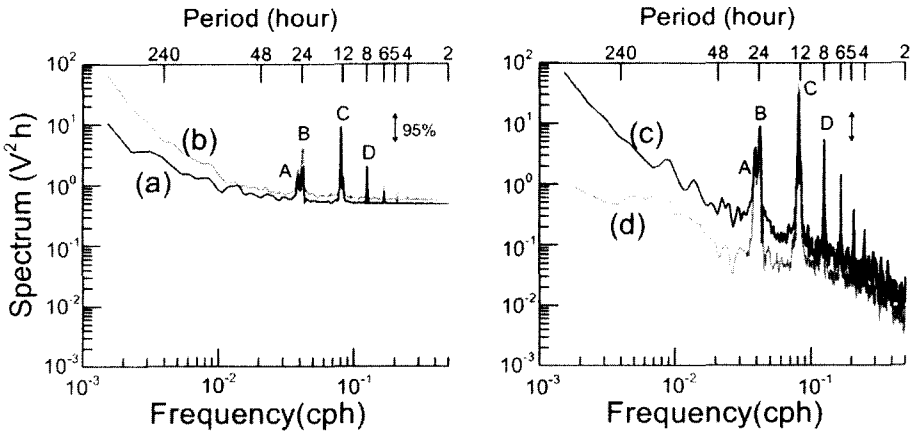


**Fig. 7.** Power Spectrum (with the 95% confidence interval) of voltages measured at (a) Hamada (dark line), (b) Pusan (light line), (c) $\Delta\Phi_{90}$ (dark line), and (d) $\Delta\Phi_{98}$ (light line). Dominant peaks are denoted by A, B, C, and D.

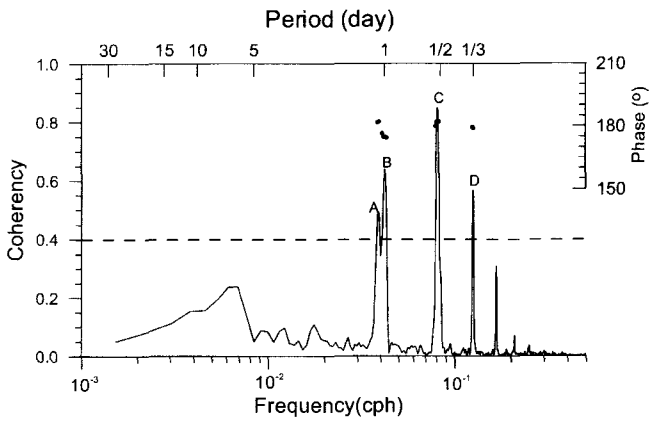


**Fig. 8.** Coherency (solid line) between voltages measured simultaneously at Hamada and Pusan in 1990 with the 95% confidence level (dashed line). Dots are cross-phase spectra corresponding to coherency higher than the 95% confidence level.

amplitude is 0.174 volt at Hamada and 0.162 volt at Pusan. The amplitude difference between these means is 3.6% of their sum and the mean phase difference is 180°. The mean amplitude of $O_1$ is 0.053 volt at Hamada and 0.051 volt at Pusan. Their difference is 1.9% of their sum and their phase difference is 186°. The standard deviation of the amplitudes relative to the mean amplitude is smaller for $M_2$ than for $O_1$.

Time series analyses of both data sets measured simultaneously at Pusan and Hamada show that tidal signals such as $M_2$ and $O_1$ are dominant and the differences between their amplitudes are less than 4% of their sums while their phase differences deviate less than 6° from 180°. These results show agreement with the simple theoretical case (in the section of Theory) even though the ground sites of the cable are not exactly on opposite sides of the flow in the Korea Strait and the bottom topography is not simple.

### *Comparison of voltage differences between 1990 and 1998*

An optical fiber cable was established for communication in 1997 and the existing submarine cable between Pusan and Hamada was abandoned. The

**Table 2.** Harmonic constants of the $M_2$ tidal constituent of the cable voltage.

| Month | Amp. (volt) | | | | Phase (°) | | | |
|---|---|---|---|---|---|---|---|---|
| | 1990 | | | 1998 | 1990 | | | 1998 |
| | Hamada | Pusan | $\Delta\Phi_{90}$ | $\Delta\Phi_{98}$ | Hamada | Pusan | $\Delta\Phi_{90}$ | $\Delta\Phi_{98}$ |
| Apr | 0.191 | 0.170 | 0.361 | 0.366 | 7 | 189 | 8 | 8 |
| May | 0.172 | 0.145 | 0.315 | 0.361 | 5 | 174 | 0 | 8 |
| Aug | 0.156 | 0.140 | 0.296 | 0.328 | 9 | 187 | 8 | 6 |
| Sep | 0.161 | 0.154 | 0.315 | 0.380 | 11 | 192 | 11 | 9 |
| Oct | 0.180 | 0.176 | 0.353 | 0.383 | 11 | 205 | 18 | 7 |
| Nov | 0.179 | 0.179 | 0.358 | 0.388 | 7 | 184 | 5 | 2 |
| Dec | 0.181 | 0.173 | 0.354 | 0.377 | 10 | 189 | 10 | 6 |
| Mean | 0.174 | 0.162 | 0.336 | 0.369 | 9 | 189 | 9 | 7 |
| SD | 0.012 | 0.016 | 0.027 | 0.021 | 2.2 | 9.3 | 5.4 | 2.5 |

**Table 3.** As in Table 2 except for $O_1$.

| Month | Amp. (volt) | | | | Phase (°) | | | |
|---|---|---|---|---|---|---|---|---|
| | 1990 | | | 1998 | 1990 | | | 1998 |
| | Hamada | Pusan | $\Delta\Phi_{90}$ | $\Delta\Phi_{98}$ | Hamada | Pusan | $\Delta\Phi_{90}$ | $\Delta\Phi_{98}$ |
| Apr | 0.030 | 0.048 | 0.078 | 0.136 | 281 | 98 | 279 | 275 |
| May | 0.082 | 0.040 | 0.122 | 0.140 | 286 | 107 | 286 | 278 |
| Aug | 0.044 | 0.052 | 0.092 | 0.108 | 292 | 82 | 276 | 278 |
| Sep | 0.041 | 0.057 | 0.097 | 0.110 | 286 | 115 | 291 | 278 |
| Oct | 0.058 | 0.066 | 0.124 | 0.129 | 297 | 110 | 293 | 284 |
| Nov | 0.072 | 0.043 | 0.115 | 0.115 | 293 | 121 | 296 | 276 |
| Dec | 0.043 | 0.052 | 0.094 | 0.115 | 307 | 107 | 296 | 285 |
| Mean | 0.053 | 0.051 | 0.103 | 0.122 | 292 | 106 | 288 | 279 |
| SD | 0.019 | 0.009 | 0.017 | 0.013 | 8.7 | 12.5 | 8.1 | 3.9 |

voltage difference between Pusan and Hamada has been measured at the Pusan Submarine Cable Relay Station using the abandoned cable since March 1, 1998. The voltage difference from March to December 1998 ($\Delta\Phi_{98}$) is compared with the voltage difference in 1990 ($\Delta\Phi_{90}$), which is obtained by subtracting the voltage measured at Pusan from that at Hamada.

There are no abrupt or long-term changes in $\Delta\Phi_{98}$ measured using the abandoned cable (Fig. 5d). The range of the short-period variations is about 1.5 volt both in $\Delta\Phi_{90}$ and $\Delta\Phi_{98}$ (Fig. 5c, d), most of which can be explained by semi-diurnal and diurnal tidal variations as can be seen in the expanded time series (Fig. 6c, d). The results of power spectral analyses indicate that $\Delta\Phi_{98}$ has peaks at the same diurnal (A, B), semi-diurnal (C), and 1/3-day (D) periods as $\Delta\Phi_{90}$ and almost the same magnitude at each peak (Fig. 7c, d). However, $\Delta\Phi_{98}$ has lower power than $\Delta\Phi_{90}$ at long periods, which implies that the high spectral power in $\Delta\Phi_{90}$ at these periods may be related to the effects of the room temperature on the voltmeter in 1990.

The harmonic analyses show that the mean amplitude of the $M_2$ signal in $\Delta\Phi_{90}$ is 0.336 volt. Its mean phase is 9°, which is the same as that at Hamada (Table 2). This phase relation is expected because the voltages at Hamada and Pusan have opposite phases at the $M_2$ frequency. In $\Delta\Phi_{98}$ the mean amplitude of the $M_2$ constituent is 0.369 volt and the phase is 7°. Thus, the mean amplitude difference between $\Delta\Phi_{90}$ and $\Delta\Phi_{98}$ is as small as 9% and the mean phase difference is just 2°. In $\Delta\Phi_{90}$ the mean amplitude at $O_1$ frequency is 0.103 volt and the phase is 288° (Table 3). In $\Delta\Phi_{98}$ the mean amplitude at $O_1$ frequency is 0.122 volt and the phase is 279°. The mean amplitude difference between these data sets is 15% and the phase difference is 9°. $M_2$ is more suitable than $O_1$ for finding the relation between the voltage and the volume transport because the former has a larger amplitude and its smaller standard deviation than the latter. It can be inferred from these concordant results using differing measuring times and methods that the relationship between observed voltage and volume transport is robust and has a small variance in time.

## CONVERSION FROM VOLTAGE TO TRANSPORT USING TIDAL SIGNALS

Simultaneously measured volume transports are needed to calibrate the voltage measurements for monitoring transport variations. However, until recently, it was not possible to obtain long-term and continuous accurate transport estimates across the Korea Strait due to high fishing activity. Therefore, tidal transports were used to estimate the conversion factor from voltage to transport in previous studies (Choi *et al.*, 1992; Choi *et al.*, 1997). The amplitude of $M_2$ tidal transport obtained by tidal models (Kang *et al.*, 1991; Choi *et al.*, 1994) or by limited current meter data (Odamaki, 1989) has a range of 5.0–5.5 $\times 10^6$ $m^3s^{-1}$ in the northeastern section of the Korea Strait. Choi *et al.* (1992) and Choi *et al.* (1997) estimated the conversion factor as 35.95 and $30.90\times10^6$ $m^3s^{-1}volt^{-1}$ using $M_2$ tidal transport of $5.5\times10^6$ $m^3s^{-1}$ and $M_2$ voltage variation of 0.154 and 0.178 volt, respectively (Table 1). Since they used the voltage variation only at Pusan measured using the in-service cable, half of the total voltage variation across the strait was compared with the tidal transport.

Recently, tidal currents were assimilated in a barotropic model for the Korea Strait (Book *et al.*, 2001). The model assimilated coastal sea level data, TOPEX/POSEIDON altimetry data, moored pressure data, and current data measured by fifteen ADCPs. Most of these ADCPs were deployed in Trawl Resistant Bottom Mounts along two lines in the Korea Strait from May 1999 to March 2000 (Perkins *et al.*, 2000). Amplitudes of tidal transports across the cable section are calculated as 4.38 and $1.79\times10^6$ $m^3s^{-1}$ for $M_2$ and $O_1$, respectively, from the assimilation model (Table 1). Conversion factors from voltage to transport can also be derived by comparing tidal amplitudes of this model-derived transport and $\Delta\Phi_{98}$. Derived conversion factors are 11.9 and 14.7 for $M_2$ and $O_1$, respectively (Table 1). As mentioned previously, the amplitude of $O_1$ in $\Delta\Phi_{98}$ has a relatively larger variance than that of $M_2$; that is, the $O_1$ signal is less stable than the $M_2$ signal. Moreover, the amphidromic point of $O_1$ is reproduced near Pusan from the tidal model (Book *et al.*, 2001). This implies that $O_1$ tidal currents are more complex than $M_2$ currents near the cable section. These complexities may explain the different conversion factors for $M_2$ and $O_1$.

The characteristic length scale of tidal currents along the Korea Strait is estimated to be about 200 km, which is close to the width of the Korea Strait. If this estimate is true, then the horizontal electric current effect along the strait on the measured voltage should be considered as described in the section of Theory. The effect can be estimated by using the characteristic downstream length scales in Equations (8) and (9). The width ($L$) of the Korea Strait, the water conductivity ($\sigma_1$), and the water depth ($H_1$) are assumed to be 200 km, 4 S $m^{-1}$, and 100 m, respectively. The conductances of the upper crust ($\sigma_2H_2$) and the land ($\tau^*$) are estimated to be 1000 S and 400 S, respectively, using conductivity values reported by Utada *et al.* (1986). $\nu_0$ is calculated to be 0.29 using (6) and $R_1/R_3$ is described as,

$$R_1/R_3 = \frac{4\tau^* L}{\pi\sigma_1 H_1 Y} \tag{10}$$

Then $\kappa$ can be calculated by (9) for various characteristic length scales ($Y$) of the motion along the strait (Table 4). The cross-stream voltage ($\Delta\Phi_V$) generated by a fixed transport will change, if $Y$ varies.

Assuming that the characteristic length scale of tidal currents in the Korea Strait is about 200 km, the cross-stream electric potential difference, $\Delta\Phi_V$, can be reduced by 27% from the local motion-induced potential difference, $\Delta\Phi_L$ (Table 4). Since the amplitude of $\Delta\Phi_V$ is 0.369 volt for $M_2$, $\Delta\Phi_L$ is estimated as 0.51 volt using (9). Comparing this $\Delta\Phi_L$ and the tidal transport for $M_2$, the conversion factor changes to $8.6\times10^6$ $m^3s^{-1}volt^{-1}$. For $O_1$, $\Delta\Phi_V$ is 0.122 volt and $\Delta\Phi_L$ is estimated as 0.17 volt. This gives a conversion factor of $10.5\times10^6$ $m^3s^{-1}volt^{-1}$. The horizontal electric current effect must be considered when using voltage to transport conversion factors derived from tidal signals. However, this effect on $\Delta\Phi_V$ becomes smaller with $Y$. Moreover, as the length scale becomes larger, $\kappa$ changes less with $Y$.

**Table 4.** The values of $\kappa$ calculated for various downstream length scales ($Y$).

| $Y$(km) | 100 | 200 | 300 | 400 | 500 |
|---|---|---|---|---|---|
| $\kappa$ | 0.42 | 0.27 | 0.20 | 0.15 | 0.13 |

## CONCLUDING REMARKS

If there are no downstream changes of velocity and conductivity, charges separated by the motion-induced electromotive force are evenly distributed along the strait. In this simple case, electric potential variations at any two points across the strait have the same amplitude and opposite phase, and their differences are proportional to the volume transport. In voltage data measured simultaneously at Pusan and Hamada in 1990 tidal signals such as $M_2$ and $O_1$ are dominant. Their amplitude differences are less than 4% of their sums and their phase differences deviate less than 6° from 180°. These results correspond to a simple theoretical case even though the ground sites of the cable are not exactly on opposite sides of the flow in the Korea Strait.

In the voltage difference ($\Delta\Phi_{90}$) obtained using the in-service cable and that ($\Delta\Phi_{98}$) measured using the abandoned cable the dominant signals appear at the same diurnal, semi-diurnal, and 1/3-day periods with almost the same magnitudes at each peak. Moreover, they have about the same amplitude and phase for the $M_2$ and $O_1$ signals. Therefore, the relationship between the observed voltage and the volume transport through the Korea Strait can be considered robust and to be maintained stably over time. The linear conversion factor from voltage to transport is estimated to be $11.9\times10^6$ $m^3s^{-1}volt^{-1}$ by comparing the tidal amplitudes of model-derived transport and voltage for $M_2$. This value changes to $8.6\times10^6$ $m^3s^{-1}$ $volt^{-1}$ when taking into consideration the horizontal electric

current effect. To obtain a more reliable and stable conversion factor from voltage to transport, the voltage should be compared with observed sub-tidal transports, which may have long downstream length scales.

## ACKNOWLEDGEMENT

The authors thank Korea Telecom and NTT of Japan for their transfer of the submarine telephone cable between Pusan and Hamada. The authors are very grateful to two reviewers (Profs. Moon-Jin Park and Jae-Chul Lee) for their helpful comments. This work was supported by OCEAN Laboratory and the Agency for Defense Development of Korea through the Underwater Acoustics Research Center (UD970022AD) in 1999-2001. This is OCEAN Laboratory contribution No. 9. J. W. Book was supported by the U.S. Office of Naval Research as part of the basic research project "Linkages of Asian Marginal Seas" under program element 0601153N (NRL-SSC contribution JA/7330/01/0068).

## REFERENCES

Bahk, K.S., 1991. Development of a voltage measuring system for the Pusan Hamada submarine cable. *J. Korean Soc. of Coastal and Ocean Engineers*, **3**: 255–260.

Book, J.W., W.J. Teague, P. Pistek, H.T. Perkins, B.-H. Choi, G. A. Jacobs, M.-S. Suk, K.-I. Chang and J.-C. Lee, 2001. Tides in the Korea/Tsushima Strait: Observation and Model Predictions. *Proceedings of the 11th PAMS/JECSS Workshop, Cheju, Korea*, 207–210.

Bowden, K.F., 1956. The flow of water through the Strait of Dover related to wind and differences in sea level. *Phil. Trans. Roy. Soc. London, A*, **248**: 517–551.

Choi, B.-H., I.K. Bang and K.H. Kim, 1994. Vertical distribution of tidal current in the Korea Strait. *J. Korean Soc. of Coastal and Ocean Engineers*, **6**: 421–438.

Choi, B.-H., K. Kim, Y.-G. Kim and K. Kawatate, 1997. Submarine cable voltage measurement between Pusan and Hamada for the years 1987~1996. *Acta Oceanographica Taiwanica*, **36**(1): 33–46.

Choi, B.-H., K. Kim, Y.-G. Kim, K.S. Bahk, J.O. Choi and K. Kawatate, 1992. Submarine cable measurements between Pusan and Hamada. *La mer*, **30**: 157–167.

Kang, S.K., S.-R Lee and K.-D. Yum, 1991. Tidal computation of the East China Sea, the Yellow Sea and the East Sea. In: Oceanography of Asian Marginal Seas, edited by K. Takano, Elsevier Oceanography Series **54**: 24–48.

Kawatate, K., A. Tashiro, M. Ishibashi, T. Shinozaki, T. Nagahama, A. Kaneko, S. Mizuno, J. Kojima, T. Aoki, T. Ishimoto, B.H. Choi, K. Kim, T. Miita and Y. Ouchi, 1991. A cross-spectral analysis of small voltage variation in a submarine cable between Hamada and Pusan with speed variation of the Tsushima Warm Current. In: Oceanography of Asian Marginal Seas, edited by K. Takano, Elsevier Oceanography Series, **54**: 207–222.

Larsen, J.C., 1992. Transport and heat flux of the Florida Current at 27°N derived from cross-stream voltages and profiling data: theory and observations. *Phil. Trans. R. Soc. London, A*, **338**: 169–236.

Larsen, J.C., R.L. Mackie, A. Manzella, A. Fiordelisi and S. Rieven, 1996. Robust smooth magnetotelluric transfer functions. *Geophys. J. Int.*, **124**: 801–819.

Longuet-Higgins, M.S., 1949. The electrical and magnetic effect of tidal streams. *Mon. Not. R. Astr. Soc.*, **16**: 285–307.

Mayer, D.A. and J.C. Larsen, 1986. Tidal Transport in the Florida Current and Its Relationship to Tidal Heights and Cable Voltages. *J. Phys. Oceanogr.*, **16**: 2199–2202.

Odamaki, M, 1989. Tides and tidal currents in the Tsushima Strait. *J. Oceanogr. Soc. Japan*, **45**: 65–82.

Perkins, H.T., W.J. Teague, G.A. Jacobs, K.-I. Chang and M.-S. Suk, 2000. Currents in Korea-Tsushima Strait during Summer 1999. *Geophys. Res. Lett.*, **27**: 3033–3036.

Sanford, T.B. and R.E. Flick, 1975. On the relationship between transport and motional electric potentials in broad, shallow currents. *J. Mar. Res.*, **33**: 123–139.

Utada, H., Y. Hamano and T. Yukutake, 1986. A two-dimensional conductivity model across Central Japan. *J. Geomagnetism and Geoelectricity*, **38**: 447–473.

Manuscript received June 19, 2001
Revision accepted December 31, 2001
Editorial handling: Jae-Hak Lee